2020 IEEE/RSJ International Conference on Intelligent Robots and Systems (IROS)
October 25-29, 2020, Las Vegas, NV, USA (Virtual)

Task-oriented Contact Adjustment in Deformable Objects Manipulation with Non-fixed Contact

Jing Huang, Yuanpei Cai, Xiangyu Chu, and K. W. Samuel Au

***Abstract*— The assumption of fixed contact between robots and deformable objects (DOs) is widely used by previous DO manipulation (DOM) studies. However, in many real-life applications, the fixed contact is inapplicable due to various factors, such as the end-effector's size limitation and DO's intrinsic material properties. In such cases, the non-fixed contact (NFC), which has not been well-investigated so far, usually demonstrates better applicability. For NFC-DOM problems, the contact condition description and adjustment are essential for the task execution. In this work, we propose a novel visual characterization method in both physical and task levels to describe the real-time contact status between the end-effector and the manipulated DO, which enables the robot to perform contact adjustment for the specific ongoing manipulative task. The simulation and experimental results are also presented to validate the effectiveness of the method.**

I. Introduction

Although important strides have been made in DOM studies in recent years, automatic DOM remains an open research problem [1]. One of the unexplored topics is the robot-DO interaction mechanism as well as its adjustment control policy. Majority of the existing automatic DOM algorithms and controllers rely on the assumption that the robot and DO have invariable fixed-point contact (FPC) during the entire manipulation process, which can work well for most occasions. However, in many real-life applications, DOM with FPC (FPC-DOM) may not always be applicable subjected to very common reasons, such as the limited size and grasping capability of the end-effector, the fragile material property of the DO, etc. To overcome the aforementioned limitations of FPC-DOM, DOM with non-fixed contact (NFC-DOM) presents different advantages and is investigated in this work, in particular, we focus on the contact characterization and active contact adjustment control strategy in NFC-DOM.

Non-fixed contact (NFC) corresponds to cases where there is no firm grasping contact between the end-effector and the manipulated DO. The variable and indeterministic contact in NFC endows the robot with more contact flexibility to meet various constraints. While on the other hand, it also poses additional challenges as contact characterization and contact adjustment become essential. In this work, we propose a novel and versatile method for real-time contact description, which enables task-oriented contact adjustment. To this end, a contact index depicting the end-effector pose w.r.t. the DO in a specific manipulation task is designed and the real-time contact description is formulated as an optimization problem.

The authors are with the Department of Mechanical and Automation Engineering, The Chinese University of Hong Kong, Hong Kong, China. {huangjing, ypcai, xychu, samuelau}@mae.cuhk.edu.hk

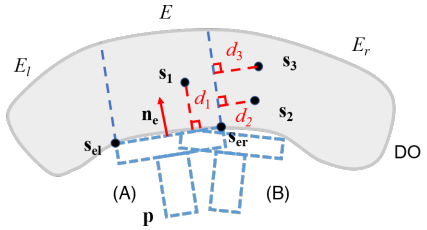

Fig. 1. Illustration of DO segmentation and end-effector representation.

This method can be further integrated with state-of-the-art deformation control approaches to compose a combined task-level controller for NFC-DOM problems.

II. Contact Description in NFC-DOM

A. System Setup and Manipulation Task

The discrete feature description of the DO is adopted here, where the visual feedback vector $\mathbf{s} = [\mathbf{s_1}^\mathsf{T}\ \mathbf{s_2}^\mathsf{T} ...\ \mathbf{s_k}^\mathsf{T}]^\mathsf{T} \in \mathbb{R}^{2k}$ stacks all the feedback points $\mathbf{s_i}$ picked on DO. The deformation of interest is described by the deformation feature vector $\mathbf{y} \in \mathbb{R}^n$, i.e.,

$$\mathbf{y} = \mathcal{F}(\mathbf{s}), \tag{1}$$

where $\mathcal{F} : \mathbb{R}^{2k} \mapsto \mathbb{R}^n$ represents the feature vector extraction function. The deformation map form the end-effector's visual representation $\mathbf{p} \in \mathbb{R}^6$ to the visual feedback vector $\mathbf{s}$ is described by the unknown mapping $\mathcal{D} : \mathbb{R}^6 \mapsto \mathbb{R}^{2k}$,

$$\delta\mathbf{s} = \mathcal{D}(\delta\mathbf{p}). \tag{2}$$

As other model-free approaches did [2]-[4], no explicit model assumption is utilized here. For NFC mechanisms, the planar contact is considered in light of its theoretical and practical importance, whose visual representation is composed of $\mathbf{p} = [\mathbf{s_{el}}^\mathsf{T}\ \mathbf{s_{er}}^\mathsf{T}\ \mathbf{n_e}^\mathsf{T}]^\mathsf{T} \in \mathbb{R}^6$, as shown in Fig. 1. The manipulation task is then framed as moving the DO so that the error norm $||\mathbf{e_y}||_2 = ||\mathbf{y} - \mathbf{y_d}||_2$ with $\mathbf{y_d}$ being the preset desired configuration, can asymptotically converge to zero.

B. Task-oriented Contact Description

Apart from the physical contact description, it is hoped that the robot is able to identify how good a specific contact state is for the ongoing manipulative task to facilitate task-oriented contact adjustment. For example, in Fig. 1, if the task involves moving feedback points $\mathbf{s_1}, \mathbf{s_2}, \mathbf{s_3}$, then configuration (B), in which the end-effector is directly placed underneath these points, will be more beneficial. In this work, the task-oriented contact index (TCI) is proposed to evaluate

978-1-7281-6211-9/20/$31.00 ©2020 IEEE

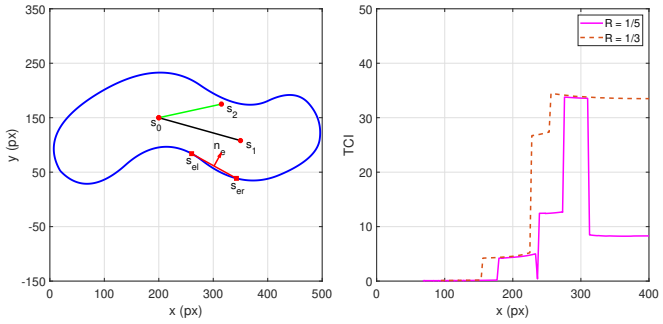

Fig. 2. Examples of TCI with different settings. TCI is calculated when the end-effector midpoint traverses the shape bottom. R is the ratio of the end-effector's length to the shape length in X-direction.

the quality or effectiveness of the current contact state for the ongoing DOM task.

Mathematically, TCI is defined as the square of the Euclidean norm of the weighted feature Jacobian $\mathbf{M} \in \mathbb{R}^n$, to assess the contact state at the task level. $\mathbf{M}$ is defined as

$$\mathbf{M}(\mathbf{y}, \mathbf{s}, \mathbf{p}) = |\frac{\partial \mathbf{y}}{\partial \mathbf{s}}| \mathbf{W}(\mathbf{s}, \mathbf{p}), \tag{3}$$

where $|\frac{\partial \mathbf{y}}{\partial \mathbf{s}}| \in \mathbb{R}^{n \times 2k}$ is the absolute Jacobian of the visual feature $\mathbf{y}$ w.r.t. the visual feedback $\mathbf{s}$. $\mathbf{W} \in \mathbb{R}^{2k}$ is the weight vector used to quantify how influential the end-effector is on feedback points. Usually, we can account for factors like distances and distribution of feedback points when constructing $\mathbf{W}$. A greater TCI indicates a better end-effector placement for the ongoing task.

C. Problem Formulation of Contact Adjustment

If the goal is to optimize the contact condition in NFC-DOM, one can formulate it as an optimization problem as follows:

$$\begin{aligned} \arg\max_{\mathbf{x_t}} \ & ||\mathbf{M}(\mathbf{y},\mathbf{s},\mathbf{p})||^2 \\ \text{s.t.} \quad & \mathcal{L}(\mathbf{p}) < \mathcal{L}_0, \\ & \mathcal{H}(\mathbf{s}) < \mathcal{H}_0. \end{aligned} \tag{4}$$

where $\mathbf{x_t} \in SE(3)$ is the end-effector's pose. $\mathcal{L}(\mathbf{p})$ is the function used to characterize the physical contact state, i.e., whether the end-effector can manipulate the DO with current physical contact condition. For planar contact, $\mathcal{L}(\mathbf{p})$ can be used to depict whether the planar contact is established. This optimization framework is also capable of involving more constraints on the task execution, such as the distribution of $\mathbf{s}$ w.r.t. $\mathbf{p}$ characterized by $\mathcal{H}(\mathbf{s})$, making it possible for the robot to perform more challenging and complicated tasks.

III. Results

A. Simulation Results

Fig. 2 shows how TCI changes when $\mathbf{p}$ traverses the bottom of an arbitrary DO contour for an angle deformation feature composed of three feedback points. There are multiple steps in the TCI curves for the feedback points enter or leave the "effective" manipulation region as $\mathbf{p}$ keeps moving. For each point, $|\frac{\partial \mathbf{y}}{\partial \mathbf{s_i}}|$ quantifies its influence on $\mathbf{y}$ and is

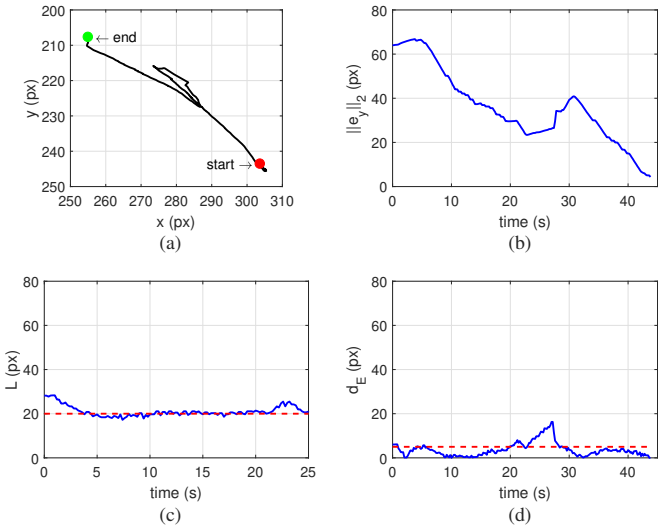

Fig. 3. Point manipulation: (a) point trajectory, (b) error norm, (c) $\mathcal{L}(\mathbf{p})$, and (d) weight distance factor d_E in $\mathbf{W}$.

determined by $\mathcal{F}$. While $\mathbf{W}$ determines how effectively or influentially the end-effector can manipulate an individual point. In the simulation, the distance-based criteria are taken when constructing $\mathbf{W}$.

B. Experimental Results

The da Vinci Research Kit (dVRK) was used as the robotic platform for our experiments. A custom-made 3D-printed planar board was utilized for NFC manipulation. A soft fabric sheet which had negligible elasticity but notable compliance was folded to serve as the DO. For deformation control, a numerical method and classical error-driven controller were implemented. We present a single point manipulation task for simplicity (Fig. 3). In the experiment, the robot could perform task-oriented contact adjustment by solving the contact optimization problem Eq. (4) when the the contact condition became unqualified, i.e., constraints in Eq. (4) were violated, to accomplish the NFC-DOM task.

IV. Conclusion

In this work, we proposed a novel contact index and optimization framework to characterize the contact state in NFC-DOM tasks, which enabled the robot to perform task-oriented contact adjustment. The effectiveness of our method were validated by the simulation and experimental results.

References

[1] J. Sanchez, J.-A. Corrales, B.-C. Bouzgarrou, and Y. Mezouar, "Robotic manipulation and sensing of deformable objects in domestic and industrial applications: a survey," *Int. J. Robot. Res.*, vol. 37, no. 7, pp. 688–716, 2018.

[2] D. Navarro-Alarcon, Y.-H. Liu, J. G. Romero, and P. Li, "Model-Free Visually Servoed Deformation Control of Elastic Objects by Robot Manipulators," *IEEE Trans. Robot.*, vol. 29, no. 6, pp. 1457–1468, 2013.

[3] Z. Hu, P. Sun, and J. Pan, "Three-Dimensional Deformable Object Manipulation Using Fast Online Gaussian Process Regression," *IEEE Robot. Autom. Lett.*, vol. 3, no. 2, pp. 979–986, 2018.

[4] F. Alambeigi, Z. Wang, R. Hegeman, Y.-H. Liu, and M. Armand, "A Robust Data-Driven Approach for Online Learning and Manipulation of Unmodeled 3-D Heterogeneous Compliant Objects," *IEEE Robotic. Autom. Lett.*, vol. 3, no. 4, pp. 4140–4147, 2018.